



Efficacy of computed tomography features in the differentiation of basal cell adenoma and Warthin tumor in the parotid gland

Yao Yu, MD,^a Wen-Bo Zhang, MD,^a Hui Yuh Soh, MM,^b Zhi-Peng Sun, MD,^c Guang-Yan Yu, MD, DDS,^d and Xin Peng, MD, DDS^d

Objective. The aim of this study was to identify computed tomography (CT) features that differentiate basal cell adenoma (BCA) from Warthin tumor (WT).

Materials and Methods. Histopathologically confirmed parotid gland tumors (57 BCAs and 83 WTs) were retrospectively reviewed. CT images were evaluated to determine location, distribution, cyst formation, size, the new vessel facing sign (VFS), and enhancement behavior including the CT attenuation of solid portions of the tumor (AST), the vessel near the tumor (AVT), and maxillary artery (AMA) on early stage 2-phase contrast CT. Tumor CT attenuation ratios (AST/AVT and AST/AMA) were calculated. Chi-square tests, independent *t*-tests, and receiver operating characteristic curve analysis were conducted.

Results. Male:female ratio, patient age, posteroinferior location, tumor size, and presence of VFS were significantly lower for BCA than WT. The average AST/AVT was significantly higher for BCA than WT. The threshold value for AST/AVT on early stage 2-phase contrast CT was 0.72 between BCA and WT, and sensitivity and specificity were 94.7% and 98.8%, respectively, as calculated by receiver operating characteristic analysis.

Conclusion. Gender ratio, age, location, size, presence of VFS, and AST/AVT value may help to differentiate BCA from WT in parotid glands on CT examination. (Oral Surg Oral Med Oral Pathol Oral Radiol 2021;132:589–596)

Parotid gland tumors represent approximately 3% of all head and neck tumors. In total, 80% to 85% of parotid tumors are benign; they consist mostly of pleomorphic adenomas (PAs), basal cell adenomas (BCAs), and Warthin tumors (WTs).¹ The preoperative imaging examinations of parotid tumors, including ultrasonography, computed tomography (CT), and magnetic resonance imaging, are important for differentiation of various types of benign parotid tumors because they have different treatment strategies and prognoses. However, the efficacy of preoperative imaging remains controversial for the diagnosis of PA, BCA, and WT. Currently, contrast-enhanced CT (CECT) techniques are widely used for the examination of parotid tumors. These techniques can provide useful information for characterization of tumors as well as their relationship to nearby structures and functional analysis through the essential information obtained through perfusion of the lesion.²

A recent study suggested that 2-phase helical CT can be useful in diagnosing salivary gland tumors.³ Some

studies have reported that most PAs (89.2%) showed highest density at the delayed phase, whereas BCA and WT showed early enhancement and washout of contrast material.^{4,5} The attenuation values in the early and delayed phases of BCA and WT were also compared and showed no statistically significant differences. The vessel facing sign (VFS) is defined as the appearance of the posterior mandibular veins nearest to the tumor. This sign has been reported to be a characteristic of WT.⁶ These lesions are mainly located at the posteroinferior lobe, which is near the posterior mandibular veins. Xu et al. reported that the traditional VFS was not significant for WT.⁷ However, when the VFS was used to determine the increase in new blood vessels adjacent to the tumor, 84% of WTs (21/25) presented with this sign, which was higher compared to the VFS in BCA (1/5, 20%). This result is controversial because of the small number of basal cell adenomas in the study. In addition, the definition of advanced VFS was vague.

In our clinical work, we have found that the attenuation values of the surrounding vessels in WTs were higher than in the tumors themselves in early phase CT.

Statement of Clinical Relevance

Image-based differential diagnosis of different parotid gland tumors is important because these neoplasms often require different surgical treatment. This research revealed that various parameters in contrast-enhanced computed tomography can differentiate basal cell adenoma from Warthin tumor.

^aAttending Doctor, Department of Oral and Maxillofacial Surgery, Peking University School and Hospital of Stomatology, Beijing, China.

^bResident, Department of Oral and Maxillofacial Surgery, Peking University School and Hospital of Stomatology, Beijing, China.

^cAssociate Professor, Department of Oral and Maxillofacial Surgery, Peking University School and Hospital of Stomatology, Beijing, China.

^dProfessor, Department of Oral and Maxillofacial Surgery, Peking University School and Hospital of Stomatology, Beijing, China.

Received for publication Aug 10, 2020; returned for revision Dec 22, 2020; accepted for publication Dec 28, 2020.

© 2021 Elsevier Inc. All rights reserved.

2212-4403/\$-see front matter

<https://doi.org/10.1016/j.oooo.2020.12.022>

Thus, CECT can depict the surrounding vessels that pass around and through the neoplasm. This was defined as the VFS in the present study. In addition, in the present investigation, the ratio of CT attenuation of the solid portion of the tumor (AST) to the vessel near the tumor (AVT; i.e., AST/AVT) was used to quantitatively analyze and evaluate the VFS. We aimed to describe and characterize the CT features, including more detailed parameters, and use them to differentiate between BCA and WT in a large patient sample population.

The objectives of this investigation were to compare BCAs with WTs regarding demographic features, clinical features, and parameters of CECT examination. The null hypothesis stated that there would be no statistically significant differences between the 2 tumor types for any of these findings.

METHODS

This study was approved by the ethics review board of Peking University School and Hospital of Stomatology. All procedures conformed to the tenets of the Declaration of Helsinki.

A retrospective search through the histopathology records and PACS (SmartIRIS, Taipei, Taiwan) imaging examination records at our institution from January 2015 to December 2018 revealed 54 patients diagnosed with 57 BCAs (20 men, 34 women; mean age 51 years old; age range 18-72 years old) and 76 patients diagnosed with 83 WTs (71 men, 5 women; mean age 60 years old; age range 38-82 years old) who underwent preoperative CECT, which was performed by using a 16-section Sensation scanner (Siemens, Erlangen, Germany). For all patients, 2-phase CT scans were obtained in the axial plane from the thoracic inlet to the inferior orbital ridge by using various models of multidetector-row CT scanners with 2.5 to 3.75 mm section thickness, field of view of 230 × 230 mm, and a matrix of 512 × 512 mm using a soft tissue algorithm. After the intravenous administration of 90 mL of iodinated contrast material into an antecubital vein at a rate of 3 mL/s with a power injector, the early phase CT scans were obtained with a scanning delay of 30 s, and the delayed imaging scans were acquired with a delay of 120 s.

All images were examined by 2 radiologists (senior qualified head and neck radiologists, each with more than 15 years of experience) who performed their evaluations independently. The following morphologic characteristics of the tumors were assessed:

- **Tumor location:** The location was divided into superficial and deep lobes of the parotid gland by the location of the retromandibular vein. WT often occurs in the posteroinferior lobe of parotid gland. To demonstrate whether BCA and WT had the same

characteristics of tumor location, the location was also divided into the posteroinferior lobe and other locations distinct from the posteroinferior lobe.

- **Tumor distribution:** Unilateral or bilateral.
- **Cyst formation in the tumor:** Yes or no, determined by consensus of the 2 radiologists.
- **Tumor size:** Image measurements were made by the radiologists using iPlan 3.0 software (Brainlab, Feldkirchen, Germany). The size and cystic components of the tumors were expressed in terms of maximal perpendicular dimension on the transverse plane in centimeters. The data used for statistical analysis were the average values of the measurements obtained by the 2 examiners.
- **Maximum diameter of the cystic component (MDC) and maximum diameter of the tumor (MDT):** Measurements were performed as described above.
- **Cystic ratio:** The ratio of MDC and MDT.
- **VFS:** Yes or no. Three-dimensional virtual models of the tumors, vessels near the tumors, and the maxillary artery were identified and created according to the different CT numbers. The VFS was determined by examining the surrounding vessels, whose attenuation values were higher than those in the vessels passing around and through the tumor (Figures 1 and 2).

For assessment of the unenhanced and contrast-enhanced attenuations of the tumors, a circular region of interest as large as possible (8-35 mm) was drawn on the soft tissue components of the lesions, excluding obvious cystic or necrotic areas. The mean CT attenuation of the region of interest as measured in Hounsfield units was acquired synchronously in iPlan 3.0. The cystic area was defined as having a CT attenuation of 20

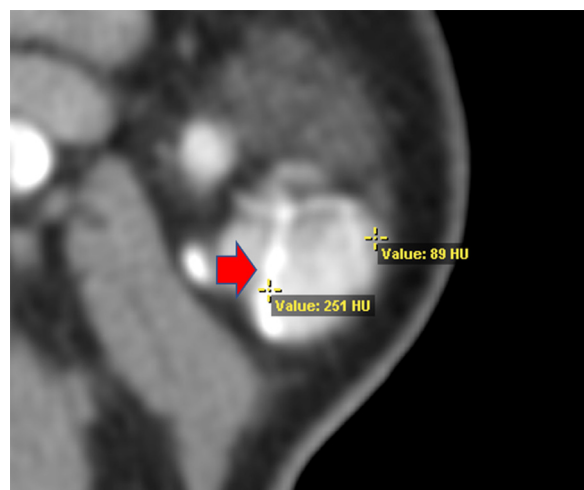


Fig. 1. A 50-year-old man with a Warthin tumor exhibiting the vessel facing sign, indicated by the red arrow. The attenuation value of the surrounding vessels (251 HU) is higher than that of the tumor (89 HU).



Fig. 2. A 50-year-old man with a Warthin tumor exhibiting the vessel facing sign. Three-dimensional imaging shows that the surrounding vessels pass around and through the tumor.

HU or less and displaying a round or ovoid shape. The following measurements were made:

- Distance between the tumor and the maxillary artery (DTA) was measured in millimeters by the 2 radiologists.
- The CT attenuation values of the AST, AVT, and the maxillary artery (AMA) in the early stage of the 2-phase contrast CT scan were measured.
- The tumor CT attenuation ratios (AST/AVT and AST/AMA) were calculated.

The measurement of the data was single-blinded for the 2 radiologists. Categorical data including patient gender and age, tumor location, distribution, cyst formation, and VFS were analyzed using chi-square tests. The independent sample *t*-test was used for analysis of the continuous numerical data. Receiver operating characteristic (ROC) curve analysis and calculation of the Youden index were performed using SPSS 20.0 (SPSS, Chicago, USA). $P \leq .05$ was considered statistically significant.

RESULTS

The number of tumors and patients, gender distribution, age, tumor location, distribution, presence or absence of cyst formation, tumor size, MDC, MDT, cystic ratio, and presence or absence of VFS of the BCAs and WTs are summarized in Table I. The gender ratio (male:female) for patients with BCAs (20:34) was significantly lower than the ratio for patients with WTs (71:5; $P < .001$). The mean age of patients with BCAs

Table I. The gender distribution, age, and general morphologic characteristics of basal cell adenomas and Warthin tumors

	Basal cell adenoma	Warthin tumor	P value
No. of tumors	57	83	
No. of patients	54	76	
Gender (male:female)	20:34	71:5	<.001
Age (±SD)	50.5 ± 12.3	59.5 ± 10.5	<.001
Location			
Superficial lobe	52	70	.231
Deep lobe	5	13	
Posteroinferior	17	64	<.001
Others	40	19	
Distribution			
Unilateral	53	69	.139
Bilateral	1	7	
Cyst formation			
Yes	19	35	.290
No	38	48	
Tumor size (±SD, cm)	1.96 ± 1.04	3.02 ± 1.03	<.001
MDC (±SD, mm)	1.25 ± 0.74	1.74 ± 1.06	.072
MDT (±SD, mm)	2.60 ± 1.29	3.61 ± 0.98	.002
Cystic ratio (SD) (MDC/MDT)	0.46 ± 0.17	0.49 ± 0.23	.697
Vessel facing sign			
Yes	9	76	<.001
No	48	7	

MDC, maximum diameter of the cystic component; MDT, maximum diameter of the tumor.

(50.5 ± 12.3 years) was also significantly lower than the age of patients with WTs (59.5 ± 10.5 years; $P < .001$). There were no statistically significant differences in location of superficial vs deep lobe distribution between the tumor types ($P = .231$), with a total of 52 of the 57 BCAs (91.2%) and 70 of the 83 WTs (84.3%) located in the superficial lobe. However, 17 BCAs were located in the posteroinferior lobe (29.8%), which was a significantly lower percentage than the 64 WTs in that lobe (77.1%; $P < .001$). No significant differences between the 2 tumors were detected regarding unilateral vs bilateral occurrence ($P = .139$) or cyst formation ($P = .290$). The mean size of BCAs (1.96 ± 1.04 cm) was significantly smaller than the mean size of WTs (3.02 ± 1.03 cm; $P < .001$). MDC was slightly smaller for BCA than WT but the difference was not significant ($P = .072$). On the other hand, MDT was significantly smaller for BCA (2.60 ± 1.29) than for WT (3.61 ± 0.98; $P = .002$). However, the cystic ratio of these measurements was not significantly different between the tumor types ($P = .697$). There were significantly fewer VFSs in BCAs (9 out of 57, or 15.8%) than in WTs (76 out of 83, or 91.6%; $P < .001$).

Results of the various CT parameters for the BCAs and WTs and their statistical comparisons are summarized in Table II. Distance between the tumor and the maxillary artery was not significantly different between

Table II. Computed tomography parameters for basal cell adenomas and Warthin tumors

	Basal cell adenoma (mean ± SD)	Warthin tumor (mean ± SD)	P value
DTA (mm)	9.7 ± 7.7	7.8 ± 6.6	.135
AST (±SD, HU)	149.43 ± 42.92	107.71 ± 21.19	<.001
AVT (±SD, HU)	145.11 ± 55.48	174.07 ± 64.94	.007
AMA (±SD, HU)	249.95 ± 47.27	247.36 ± 50.03	.759
AST/AVT	1.11 ± 0.33	0.53 ± 0.18	<.001
AST/AMA	0.61 ± 0.18	0.45 ± 0.11	<.001

CT, computed tomography; DTA, distance between the tumor and the maxillary artery; AST, CT attenuation of the solid portion of the tumor; AVT, CT attenuation of the vessel near the tumor; AMA, CT attenuation of the maxillary artery.

the 2 tumor types ($P = .135$). BCA showed significantly greater mean Hounsfield units for AST (149.43 ± 42.92) compared to WT (107.71 ± 21.19 ; $P < .001$). However, AVT values were significantly lower for BCA (145.11 ± 55.48) than for WT (174.07 ± 64.94 ; $P = .007$). The difference in AMA for BCA (249.95 ± 47.27) and WT (247.36 ± 50.03) was not significant ($P = .759$). BCA values for AST/AVT (1.11 ± 0.33) and AST/AMA (0.61 ± 0.18) were both significantly greater than the values for WT (0.53 ± 0.18 and 0.45 ± 0.11 , respectively; $P < .001$ for both comparisons).

All BCAs and WTs were painless, slowly growing, enlarged masses with well-circumscribed borders, as noted in the patients' records. One patient had bilateral BCAs, including 1 in the posteroinferior lobe of the right parotid gland and 1 in the deep lobe of the left parotid gland. The bilateral BCAs displayed different degrees of enhancement (Figure 3). In the right BCA, the AST and AVT were 127 and 122 HU, respectively (Figure 4) with AMA of 294 HU. For the left BCA, the AST and AVT were 186 and 143 HU, respectively (Figure 5),

with AMA of 294 HU. Additionally, 2 patients with BCAs had 2 lesions in the same parotid gland, and a similar enhancement behavior was observed (Figures 6 and 7). In 7 patients, WTs were bilateral, and the AST, AVT, and AMA for the tumors of the left parotid gland were not significantly different from the values for the right-sided lesions. Examples of WTs with VFS and small AST/AVT values are provided in Figures 8 and 9.

ROC curves were generated for AST, AVT, AST/AVT, and AST/AMA for the ability of these values to distinguish between BCA and WT (Figure 10). The AST threshold was 129.5 HU between BCA and WT; sensitivity and specificity were 73.7% and 88.0%, respectively. The AVT threshold was 24.5 HU between BCA and WT; sensitivity and specificity were 100% and 8.5%, respectively. The AST/AVT threshold was 0.72 between BCA and WT; sensitivity and specificity were 94.7% and 98.8%, respectively. The AST/AMA threshold was 0.55 between BCA and WT; sensitivity and specificity were 63.2% and 86.7%, respectively. The Youden indices of AST, AVT, AST/AVT, and AST/AMA were 0.616,

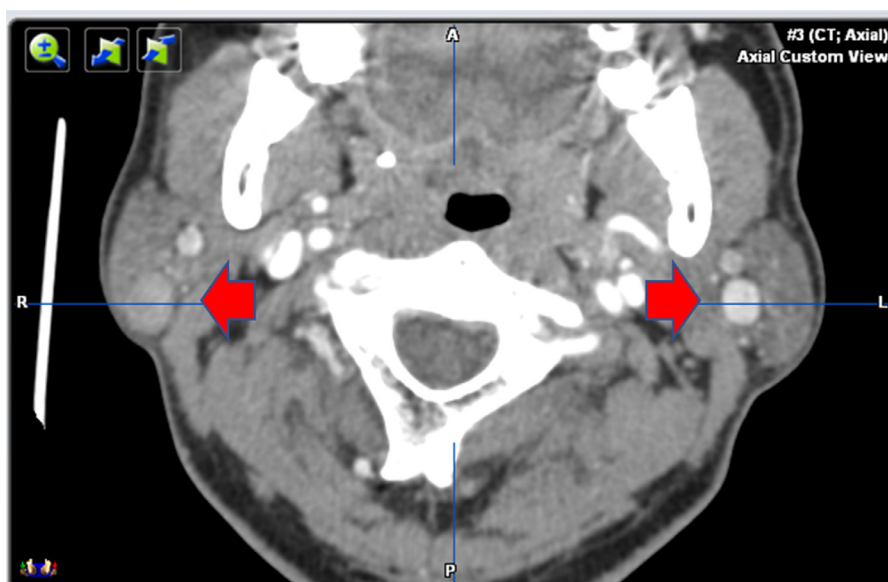


Fig. 3. A 47-year-old man with 2 basal cell adenomas (BCAs) in the bilateral parotid glands. The bilateral BCAs displayed different degrees of enhancement. The red arrows indicate the round, well-circumscribed BCAs.

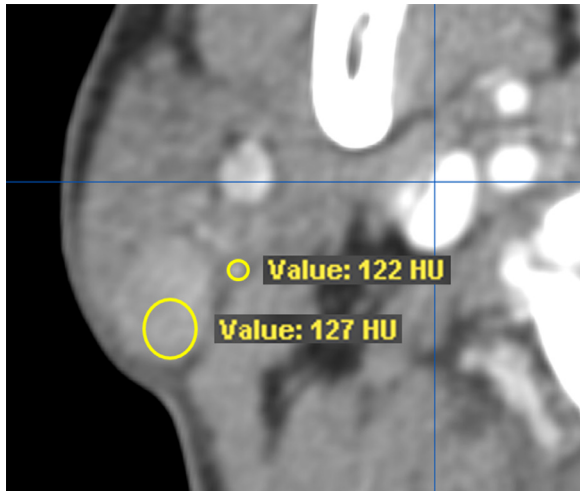


Fig. 4. A 47-year-old man with 2 basal cell adenomas in the bilateral parotid glands. For the right basal cell adenoma, the solid portion of the tumor is shown, the vessels near the tumor are marked, and the AST (127 HU) and AVT (122 HU) values are indicated.

0.084, 0.935, 0.499, respectively (Table III). Complete CT scan volumes depicting 1 BCA and 1 WT are included for examination in the 3D viewer.

DISCUSSION

Benign adenomas account for 65.6% of salivary gland tumors.⁸ Since 1991, the World Health Organization has defined basal cell adenoma as a histologically distinct entity that is characterized by an abundant basal cell layer and distinctive basement membrane-like structure.⁹ The basal cell adenoma is divided into 4 histologic subtypes, including solid, tubular, trabecular,

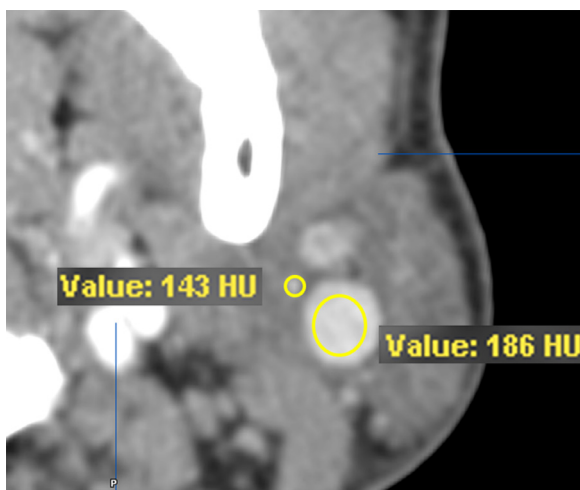


Fig. 5. A 47-year-old man with 2 basal cell adenomas in the bilateral parotid glands. For the left basal cell adenoma, the solid portion of the tumor is shown, the vessels near the tumor are marked, and the AST (186 HU) and AVT (143 HU) values are indicated.

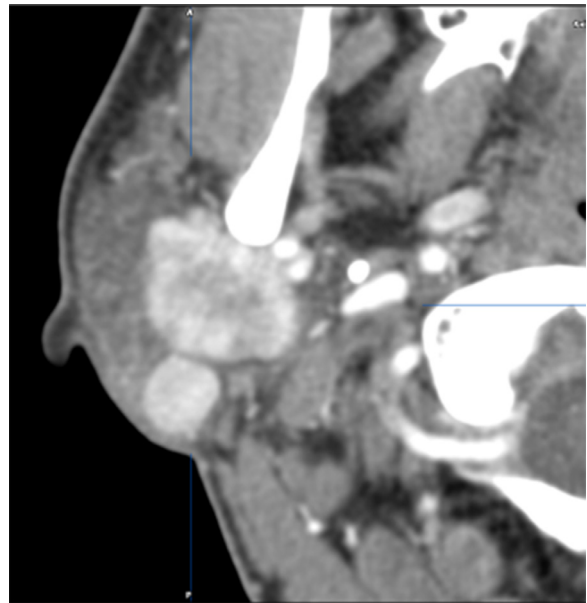


Fig. 6. A 46-year-old woman with 2 basal cell adenomas in the right parotid gland with enhancement behavior similar to that depicted in Figures 4 and 5.

and membranous, with the solid subtype being the most frequent form and the membranous subtype having a high recurrence rate.^{10,11}

Although BCA accounts for approximately 1% to 2% of all salivary gland epithelial tumors, it is the third most common type of benign parotid tumor after PA and WT.^{11,12} A painless, slowly growing, asymptomatic, freely movable parotid mass is the most common clinical manifestation of BCA. Research has demonstrated a female predominance in BCA and a male predominance in WT.^{13,14} Our analysis agreed with these

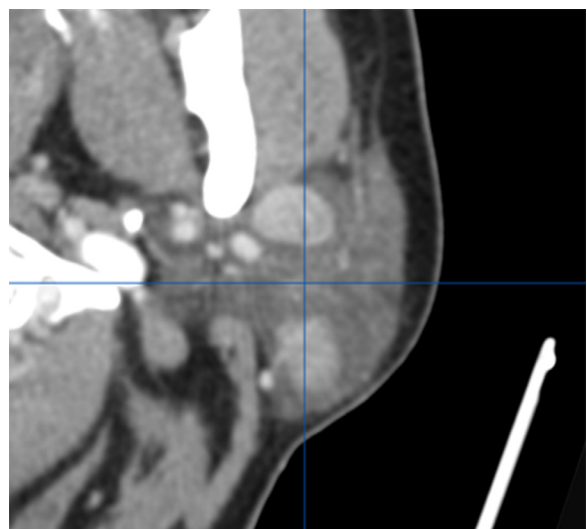


Fig. 7. A 57-year-old man with 2 basal cell adenomas in the left parotid gland with enhancement behavior similar to that depicted in Figures 4 and 5.

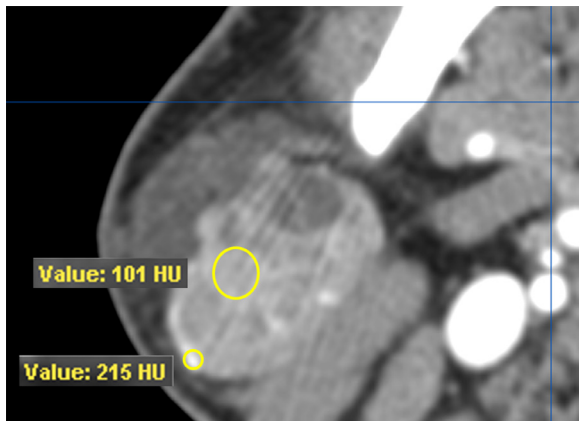


Fig. 8. The vessel facing sign of a Warthin tumor. The attenuation value of the surrounding vessels (215 HU) is higher than that of the tumor (101 HU). The value for solid portions of the tumor/vessel near the tumor is 0.47.

previous studies, revealing a significantly greater male:female ratio for WT. WT is more common in elderly men than in women and can be multifocal and bilateral in 10% to 15% of patients.^{15,16} In our study, patients with WT were significantly older than patients with BCA, and 7 patients had bilateral WTs. According to previous reports, most BCAs are unilateral.^{17,18} However, Suzuki et al. reported a rare case of bilateral parotid BCAs that showed different enhancement behaviors.¹⁸ This previous study reviewed 72 cases of bilateral parotid tumors, of which 42% were WTs, 22% were PAs, and 6.9% were BCAs. In our investigation, only 1 patient had bilateral parotid BCAs.

In general, BCAs are usually assumed to be small tumors, less than 3 cm in their greatest dimension, and generally smaller than PAs and WTs.¹⁹ The same trend was seen in our study. The mean maximum diameter of the BCAs (1.96 ± 1.04 cm) was significantly smaller

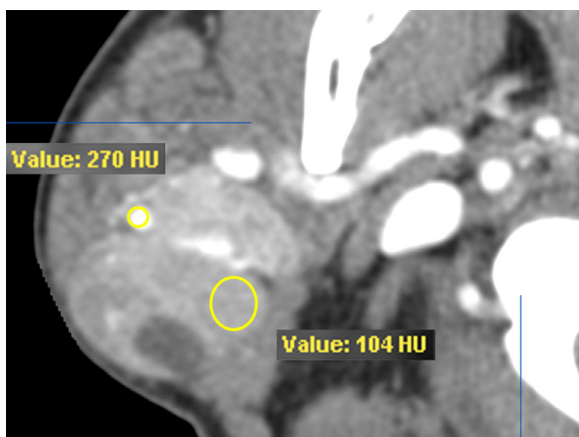


Fig. 9. The vessel facing sign of a Warthin tumor. The attenuation value of the surrounding vessels (270 HU) is higher than that of the tumor (104 HU). The value for solid portions of the tumor/vessel near the tumor is 0.38.

than that of the WTs (3.02 ± 1.03 cm). According to previous reports, cyst formation is a main histopathological feature for BCA and WT.^{14,16} The cystic ratio of BCA was significantly higher than that of PA in 1 investigation.²⁰ However, we observed no significant difference in cystic ratios between BCA and WT.

Our research revealed that BCA had significantly greater mean values for AST compared to WT. However, the parameter of AST is too unstable to be used for diagnosis, even if bilateral parotid tumors occur in the same patient. Some studies have reported that most pleomorphic adenomas (89.2%) showed highest radiodensity in the delayed phase of CECT, whereas BCAs and WTs showed early enhancement and washout of contrast material.^{4,5} The attenuation values in the early and delayed phases between BCAs and WTs were also compared in those studies and showed no statistically significant differences. Compared to AST, which represents the enhancement degree, AST/AVT and AST/AMA are more objective, with no influence from AVT and AMA, representing the vascularity and perfusion of the tumor with the same blood supply conditions. The value of AST/AVT is the quantization of VFS. In our study, the AST/AVT threshold was 0.72 between BCA and WT; sensitivity and specificity were 94.7% and 98.8%, respectively. The Youden index of AST/AVT was 0.935. According to our ROC results, the AST/AVT and VFS could be used for differentiating BCAs from WTs in parotid glands with very high sensitivity and specificity values.

Previous reports have attempted to correlate imaging characteristics of salivary gland tumors with histopathologic features.^{2,8,12,21} Many studies have described WTs as having an intermediate level of vascularization, including an extensive network of small, leaky blood vessels within the tumor, which could explain the rapid washout of contrast agent from the tumor and decreased enhancement seen on delayed-phase scans.^{2,21} Some research has reported that BCAs showed characteristically numerous endothelial-lined vascular channels, in which small capillaries and venules are prominent within the microcystic areas of the adenoma; this can explain early enhancement with a subsequent decrease in attenuation.^{8,12} In our study, BCAs and the nearby vessels had similar CT attenuation, which indicated that BCAs had abundant capillary networks. The CT attenuation of WTs was lower than that of surrounding vessels, so we could see the surrounding vessels pass around and through the tumor. This demonstrated that WTs may have lesser degrees of vascularization compared to BCAs.

A limitation of the present study was that we did not perform a radiologic-pathologic correlation of the individual tumors, which might explain the differences in the attenuation characteristics between BCAs and WTs.

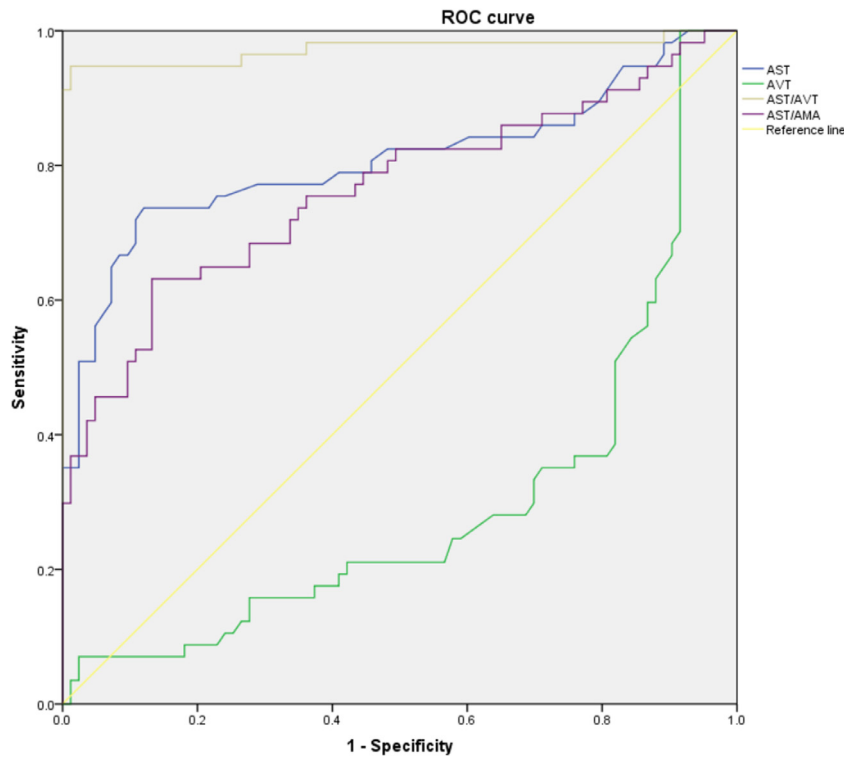


Fig. 10. The receiver operating characteristic curves for the diagnostic values of solid portions of the tumor (AST), vessel near the tumor (AVT), solid portions of the tumor/vessel near the tumor (AST/AVT), and solid portions of the tumor/maxillary artery (AST/AMA).

Table III. The cutoff point, sensitivity, specificity, and Youden index for AST, AST/AVT, and AST/AMA

	Cutoff point	Sensitivity (%)	Specificity (%)	Youden index
AST	129.5 HU	73.7	88.0	0.616
AVT	24.5 HU	100.0	8.5	0.084
AST/AVT	0.72	94.7	98.8	0.935
AST/AMA	0.55	63.2	86.7	0.499

CT, computed tomography; AST, CT attenuation of the solid portion of the tumor; AVT, CT attenuation of the vessel near the tumor; AMA, CT attenuation of the maxillary artery.

CONCLUSION

Gender ratio, patient age, location in the posteroinferior lobe, size of the tumor, the vessel facing sign, and AST/AVT on early stage 2-phase contrast CT may help differentiate BCAs from WTs in parotid glands. The AST/AVT is highly sensitive and specific and could provide a reliable means of differential diagnosis for BCAs and WTs.

ACKNOWLEDGMENT

We thank Elixigen Company for English language editing.

FUNDING

This work was supported by Key Research and Development Program of Ningxia Hui Autonomous Region (2018 BEG02012) and National Key Research and Development Project (2019 YFF0302400).

REFERENCES

1. Stenner M, Klussmann JP. Current update on established and novel biomarkers in salivary gland carcinoma pathology and the molecular pathways involved. *Eur Arch Otorhinolaryngol.* 2009;266:333-341.
2. Woo SH, Choi DS, Kim JP, et al. Two-phase computed tomography study of Warthin tumor of parotid gland: differentiation from other parotid gland tumors and its pathologic explanation. *J Comput Assist Tomogr.* 2013;37:518-524.
3. Lev MH, Khanduja K, Morris PP, Morris PP, Curtin HD. Parotid pleomorphic adenomas: delayed CT enhancement. *Am J Neuro-radiol.* 1998;19:1835-1839.
4. Reginelli A, Clemente A, Renzulli M, et al. Delayed enhancement in differential diagnosis of salivary gland neoplasm. *Gland Surg.* 2019;8:S130-S135.
5. Lee JY, Kim HJ, Kim YK, Cha J, Kim ST. Basal cell adenoma and myoepithelioma of the parotid gland: patterns of enhancement at two-phase CT in comparison with Warthin tumor. *Diagn Interv Radiol.* 2019;25:285-290.
6. Burke CJ, Thomas RH, Howlett D. Imaging the major salivary glands. *Br J Oral Maxillofac Surg.* 2011;49:261-269.

7. Xu ZF, Yong F, Yu T, et al. Different histological subtypes of parotid gland tumors: CT findings and diagnostic strategy. *World J Radiol.* 2013;28:313-320.
8. Jang M, Park D, Lee SR, et al. Basal cell adenoma in the parotid gland: CT and MR findings. *Am J Neuroradiol.* 2004;25:631-635.
9. Seigert G, Sobin LH. *Histological typing of salivary gland tumors.* World Health Organization International Histological Classification of Tumors. 2nd ed. Berlin, Germany: Springer; 1991:20-21.
10. Lee DK, Chung KW, Baek CH, Jeong HS, Ko YH, Son YI. Basal cell adenoma of the parotid gland: characteristics of two-phase helical computed tomography and magnetic resonance imaging. *J Comput Assist Tomogr.* 2005;29:884-888.
11. Chawla AJ, Tan TY, Tan GJ. Basal cell adenomas of the parotid gland: CT scan features. *Eur J Radiol.* 2006;58:260-265.
12. Okahara M, Kiyosue H, Matsumoto S, et al. Basal cell adenoma of the parotid gland: MR imaging findings with pathological correlation. *Am J Neuroradiol.* 2006;27:700-704.
13. Nagao K, Matsuzaki O, Saiga H, et al. Histopathologic studies of basal cell adenoma of the parotid gland. *Cancer.* 1982;50:736-745.
14. Takeshita T, Tanaka H, Harasawa A, Kaminaga T, Imamura T, Furui S. CT and MR findings of basal cell adenoma of the parotid gland. *Radiat Med.* 2004;22:260-264.
15. Howlett DC, Kesse KW, Hughes DV, Sallomi DF. The role of imaging in the evaluation of parotid disease. *Clin Radiol.* 2002;57:692-701.
16. Eveson JW, Cawson RA. Salivary gland tumours. A review of 2410 cases with particular reference to histological types, site, age and sex distribution. *J Pathol.* 1985;146:51-58.
17. Issing PR. Bilateral basal cell adenoma of the parotid gland and multiple cylindromas of the skin—is there a syndromal coincidence? *Laryngorhinootologie.* 1999;78:155-159.
18. Suzuki S, Okamura H, Ohtani I. Bilateral parotid gland basal cell adenomas. Case report. *ORL J Otorhinolaryngol Relat Spec.* 2000;62:278-281.
19. Habermann CR, Arndt C, Graessner J, et al. Diffusion-weighted echo-planar MR imaging of primary parotid gland tumors: is a prediction of different histologic subtypes possible? *Am J Neuro-radiol.* 2009;30:591-596.
20. Mukai H, Motoori K, Horikoshi T, et al. Basal cell adenoma of the parotid gland; MR features and differentiation from pleomorphic adenoma [e-pub ahead of print]. *Dentomaxillofac Radiol.* 2016. <https://doi.org/10.1259/dmfr.20150322s>.
21. Martinoli C, Derchi LE, Solbiati L, Rizzato G, Silvestri E, Giannoni M. Color Doppler sonography of salivary glands. *Am J Roentgenol.* 1994;163:933-941.

Reprint requests:

Prof. Xin Peng, MD, DDS
Department of Oral and Maxillofacial Surgery
Peking University School and Hospital of Stomatology
22# Zhongguancun South Avenue
Beijing 100081
China
Pxpengxin@263.net